Zero-Baseline Measurements for Relative Positioning in Vehicular Environments

Fabian de Ponte Müller, Alexander Steingass and Thomas Strang
German Aerospace Center - DLR
Institute of Communications and Navigation
Wessling, Germany
Email: fabian.pontemueller@dlr.de

***Abstract*—**

Forward collision warning systems, lane change assistants or cooperative adaptive cruise control are examples of safety relevant applications that rely on accurate relative positioning between vehicles. Current solutions estimate the position of surrounding vehicles by measuring the distance with a RADAR sensor or a camera system. One promising approach to extend the perception range of these sensors is the exchange of GNSS raw data measured from a vehicle to a set of satellites by using a inter-vehicle communication link. The aim of this approach is to cancel correlated errors in both receivers and thus achieving a better relative position estimate. The present paper shows the potential of this differential approach by showing the results of a series of zero-baseline experiments conducted in a simulated environment. The impact of uncorrelated errors that are not canceled out by differentiation, such as noise and multipath, is analyzed in depth and verified by simulations. The results show that in clear sky conditions and in absence of multipath propagation, the baseline of a vehicle can be estimated using GNSS pseudorange double differences with less than one meter of error. Multipath might severely degrade this performance, even in the case of a zero-baseline experiment.

I. Introduction

Advanced Driver Assistance Systems (ADAS) play an important role in increasing the safety on today's roads while the knowledge about other vehicle's position is a fundamental prerequisite for numerous safety critical applications in the Intelligent Transportation Systems (ITS) domain. As an example forward collision warning (FCW) systems, lane change assistants or adaptive cruise control (ACC) are examples of safety relevant applications that rely on accurate relative localization of surrounding vehicles. While FCW requires precise position and dynamic behavior of vehicles driving immediately in front, lane change assistants additionally need to localize neighboring vehicles behind or next to the ego vehicle. ACC systems on the other hand, not only need to localize the vehicle driving immediately in-front but also other vehicles ahead. This way these systems are able to better predict the platoon dynamics, react comfortably to sudden speed variations ahead and decrease the inter-vehicle distance.

Current solutions estimate the position of surrounding vehicles by measuring the distance with a RADAR, laser scanner or a camera system. In the last years RADAR sensors are rapidly decreasing in price and can be found even in medium-range compact cars. While their along track resolution is quite high, they lack a good angular resolution. Stereo vision systems, on the other hand, lack sufficient depth information at relatively good cross accuracy. Laser scanners outperform both at a higher cost [1]. However, all three solutions have a limitation in their perception range, as all of them can only detect objects in their line-of-sight (LOS).

The limited perception range of these sensors can be extended and enhanced by the use of cooperative approaches. In recent year big steps in the standardization of inter-vehicle communication have been achieved in Europe, North America and Japan. The standards IEEE802.11p or ITS-G5 allow to exchange information directly between vehicles up to a range of several hundreds of meters.

The European Telecommunications Standards Institute (ETSI) is currently working on the definition of different safety critical messages for the European Car-to-Car technology. Each vehicle will transmit periodically Cooperative Awareness Messages (CAM) [2] containing basic information such as position, speed and heading. The global coordinates are used by a vehicle to estimate its neighbors' positions. The own coordinates might be estimated using a Global Navigation Satellite System (GNSS), like the American GPS System or the future European Galileo System. This estimate can be additionally enhanced by supporting it with on-board inertial sensors or odometers.

A further possibility, though not standardized, is to exchange the GNSS raw measurements among the vehicles and estimate the baseline vector between the receiver antennas by differentiation. This approach is analogous to Differential GPS (DGPS), where a static base station transmits correction data to nearby located rover stations. However, in the raw GNSS differential approach for vehicles none of the nodes has the predominant role of the base station. The advantage of a raw GNSS differential approach is that correlated errors in both receivers are expected to cancel out.

This paper aims at analyzing this raw GNSS differential approach in different scenarios. A series of zero-baseline measurements both, static and dynamic, have been performed in a controlled environment. In a zero-baseline experiment two GPS receivers are connected to the same antenna and thus yielding a true baseline of zero meters. A Spirent GNSS Constellation Simulator System has been used for verifying the cancellation of common errors and the propagation of uncorrelated errors. As a motivation Fig. 1 shows the pseudorange double differences to the satellites in view in a zero-baseline experiment during a trip on a rural road. From 50 s to 150 s the vehicle drives through a small village, while from 150 s

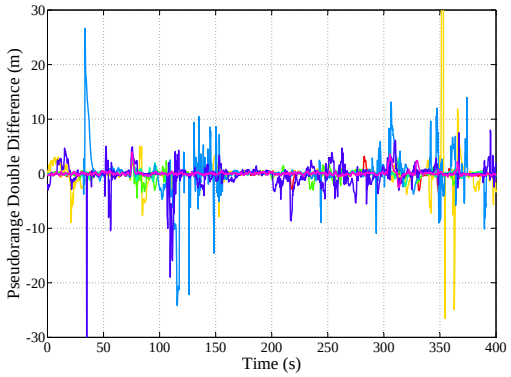

Fig. 1. Pseudorange double differences during a 400 s trip in a rural environment with a zero-baseline setup. Each color represents the double difference between a different satellite and the common satellite. In the ideal case the double differences are zero. The experiment reveals errors above 10 m. These errors have a direct impact on the baseline estimate.

the vehicle drives in an open area next to fields. However, at 200 s trees at both sides of the road provoke partial shadowing of the satellites.

In the absence of errors the double difference pseudorange measurements in a zero-baseline experiment must be equal zero. It could be argued that multipath and noise might be correlated in both receivers and also be canceled out by differentiation. Fig. 1, however, reveals large errors above 10 m when obstacles next to the road are present. This paper will analyze and quantify these errors.

The experiments show that the proposed pseudorange double differencing technique yields an unbiased estimate of the baseline in the absence of multipath propagation. While common atmospheric errors are found to cancel out correctly, multipath propagation, however, has shown to produce errors far above 10 m. The technique is able to correctly cope with dynamic stress situations that can be encountered in the road environment.

This paper is structured as follows: The following section presents related work of other groups stating shortly their contribution, their assumptions and their results. The third section describes the pseudorange differencing algorithm for estimating the baseline between two vehicles. Synchronization, noise, multipath and communication load are aspects that are specially addressed in successive subsections. Section IV describes the differencing experiments that have been performed along with the results that have been retrieved. Finally, Section V presents the conclusions of this work.

II. Related Work

The idea of differencing GNSS measurements is known since the early years of GPS. Differential GPS was born as the idea to overcome the random satellite clock error and ephemeris data truncation to artificially decrease the system's accuracy for civil users, also known as Selective Availability (SA). In DGPS a receiver located at a known position (base station) can determine the artificial offset on the range towards each satellite and send this information to other receivers (rover). Since SA is an error common to all receivers the broadcasted offset could be directly used to correct each pseudorange prior calculating the absolute position.

A series of research groups have proposed the concept of pseudorange differentiation for vehicles by moving from the classic base-station/rover setup for absolute position towards a two-rover for relative position estimation. Richter et al. introduce a relative localization approach on the basis of the exchange of GNSS pseudorange data in [3]. They formulate the mathematical problem but their work is not backed by real world measurements. In [4], Alam et al. present a tight integration approach, where pseudorange observations from two vehicles are subtracted from each other. This "cooperative positioning" approach yields a standard deviation error of 3.4 [meters] for a 12 minute run in mainly sub-urban environment. Here the uncorrelated errors not removed by double differencing are treated as observation noise. Yang et al. estimate the baseline between the vehicles using a Weighted Least Squares algorithm and weighting each pseudorange according to the received carrier to noise ratio ($\frac{C}{N_0}$) [5]. Their approach achieves an average distance error of around 3 meters over several thousand samples. Although the effect of the environment and multipath have the largest error contributions they stay unaddressed.

Zero-baseline experiments have been conducted for various purposes by different groups. In general it is assumed that multipath effects cancel out in a zero baseline experiment. Han et al. [6] propose a relative positioning system for vehicles based on pseudorange single differences. They assume similar uncorrelated error in both receivers and state that their solution is unbiased. Their experiments are performed on a open-sky sports field with a robotic vehicle equipped with two antennas placed next to each other. They assume in this setup a baseline of zero length as their ground truth. Yang compares two methods for calculating the absolute position for a DGPS system [7]. Unfortunately the measuring environment is not described in order to conclude if multipath could have been indeed discarded. The figures contain slow varying effects that cannot be assumed to be noise. García et al. perform different zero baseline experiments on the roof of a building. GNSS carrier phase measurements are extrapolated with Doppler measurements to account for the non-synchronization of different receivers [8].

In [9] Alam et al. present a cooperative positioning approach based on pseudorange double differences. In their approach noise and multipath at each channel is modeled together as an independent Gaussian error. The variance of this error is considered the same for each channel. Yang et al. [5] propose a weighted least squares method with pseudorange double differences to estimate a baseline between two antennas. Multipath errors are not modeled explicitly and are assumed not to be severe. Experimental results with static 3 meters and 8 meters baseline on a rooftop yield baseline length errors of up to 40 meters. They mention the problem of non-synchronization of measurement in two receivers, however, they do not explicitly solve it. Zhenhua et al. formulate a Bayesian fusion of an Inertial Navigation System (INS) with GPS for absolute positioning where the multipath contributions on each pseudorange are explicitly modeled [10] using time correlation constants from [11], [12], and [13]. Marchand et al.

characterize the multipath contribution on code and Doppler in dense urban environments by using a double difference based method [14]. They assume the availability of a base station in a multipath environment and one uncorrupted common satellite.

A number of groups have addressed the relative positioning problem of vehicles by solving differenced carrier phase ambiguities rather than using differenced pseudorange techniques [15], [16] , [17], [18]. The potential of this approach comes from the fact that noise in the phase-locked loop (PLL) is smaller by several orders of magnitude [13]. In order to determine the range towards the satellite the integer number of cycles has to be resolved. This task is specially difficult in vehicular environments due to signal disturbances, satellite blockage and multipath, which lead to cycle slips that will reset the resolution algorithm.

III. Pseudorange Differencing

The pseudorange differencing approach for relative positioning of vehicles relies on the double differentiation of pseudorange measurements. A pseudorange is an estimation of the distance (range) between the antennas of a GNSS satellite orbiting the Earth and a GNSS receiver on the ground. The range is attained by measuring the propagation time through the atmosphere of a signal transmitted by the satellite. Since a receiver is usually equipped with an inexpensive, inaccurate and unsynchronized oscillator, the measured distance is offset by an unknown amount. Additionally, the pseudorange is also corrupted by a series of errors produced at the satellite, the atmosphere or the receiver. The measured pseudorange ρ_i^k of a receiver i towards a satellite k can be modeled as follows:

$$\rho_i^k = R_i^k + \tau_{error} \cdot c \tag{1}$$

where R_i^k is the true receiver-to-satellite geometric range in meters, c is the speed of light, and τ_{error} are the pseudorange errors in seconds. The pseudorange errors are divided in different terms corresponding to the different error sources:

$$\tau_{error} = \tau_{sat} + \tau_{user} + \tau_{ephem} + \tau_{ion} + \tau_{trop} + \tau_{mp} + \tau_{\epsilon} \tag{2}$$

where:

- **Satellite Clock Error** (τ_{sat}): This term represents the error in the signal transmission time due to the satellite on-board clock. Each satellite is equipped with an atomic clock. Although atomic clocks are highly accurate, their errors are large enough to require correction and must be taken into account. The satellite clock error is typically less than 1ms and varies slowly.
- **Receiver Clock Error** (τ_{user}): Likewise, the receiver clock error must be included in the pseudorange error model. Receivers incorporate a quartz crystal oscillator that is far less accurate than the atomic clocks on board of the satellites. This error also includes the instrumental delay due to antenna, cable and filters.
- **Ephemeris Error** (τ_{ephem}): To calculate the receiver position the position of each satellite needs to be known. The calculation of satellite position is made by using orbital parameters broadcasted in the ephemeris data. Errors in satellite position when calculated from the ephemeris data are represented as an additional delay error term in the measured pseudorange.
- **Tropospheric Error** (τ_{trop}): The lower part of the Earth's atmosphere is composed of dry gases and water vapor which produce a delay error in the GNSS signal's propagation time in comparison to a vacuum environment. Thus, the measured pseudorange is larger than the correct value. This error depends on the path the signal has to travel through the atmosphere and therefore depends on the satellite elevation angle.
- **Ionospheric Error** (τ_{ion}): The ionosphere consists of gases that are ionized by solar radiation. The ionization produces clouds of free electrons that act as a dispersive medium for GNSS signals in which propagation velocity is a function of frequency. Ionospheric delay error varies over time in a daily cycle and, just as well as the tropospheric error, are highly dependent of the satellite elevation angle.
- **Multipath Error** (τ_{mp}): Objects in the vicinity of a receiver antenna may cause reflections of GNSS signals resulting in one or more secondary propagation paths. These secondary-path signals always have a longer propagation time and can significantly distort the amplitude and phase of the direct-path signal. In case the LOS component is blocked by the environment the correlators might track a secondary path causing a large error in the estimation.
- **Non-modeled Error** (τ_{ϵ}): This term colllects all the non-modeled errors.

A single difference measurement $\Delta\rho_{ij}^k$ is obtained by subtracting the pseudorange measurements from two different receivers referred to the same satellite k. A single differenced pseudorange measurement can be expressed therefore in the following way:

$$\Delta\rho_{ij}^k = \Delta R_{ij}^k + \Delta\tau_{error} \cdot c \tag{3}$$

where the symbol Δ denotes the difference between the corresponding terms in the two receivers i and j. ΔR_{ij}^k is the projection of the baseline in direction to satellite k and is the term we are interested in. The error term $\Delta\tau_{error}$ represents the difference of the error terms between receivers. Under a close proximity assumption the terms τ_{ion}, τ_{trop} and τ_{ephem} are nearly canceled out with the single difference operation, as well as the satellite clock error τ_{sat} that is canceled out completely. The remaining pseudorange error terms are divided in different terms corresponding to the different error sources:

$$\Delta\tau_{error} \approx \Delta\tau_{user} + \Delta\tau_{mp} + \Delta\tau_{\epsilon} \tag{4}$$

By subtracting two single differences towards two different satellites k and l a double difference measurement $\nabla\Delta\rho_{ij}^{kl}$ is computed. With this procedure the common error to both satellites is canceled. This is the case for the user clock error τ_{user}. A double difference pseudorange measurement is expressed in the following way:

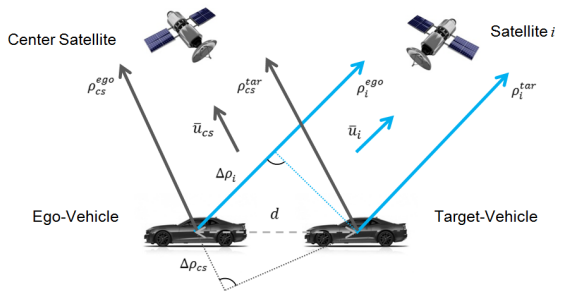

Fig. 2. Satellite-based Relative Positioning using Double Differences

$$\nabla\Delta\rho_{ij}^{kl} = \nabla\Delta R_{ij}^{kl} + \nabla\Delta\tau_{error} \cdot c \tag{5}$$

where the symbol $\nabla\Delta$ denotes the difference between the corresponding terms in the two single differences. $\nabla\Delta R_{ij}^{kl}$ is the projection of the baseline in differenced direction to satellites k and l.The error term $\nabla\Delta\tau_{error}$ represents the remaining differential error term between two receivers and two satellites:

$$\nabla\Delta\tau_{error} \approx \nabla\Delta\tau_{mp} + \nabla\Delta\tau_{\epsilon} \tag{6}$$

The remaining errors are mainly multipath and non-modeled errors like thermal noise and interferences. It should be noticed that, while common errors terms are nearly canceled out by differencing, uncorrelated error terms increase the noise variance within this operation likewise.

Fig. 2 shows the geometric relationship between the vehicles and the satellites. The baseline $\tilde{\mathbf{b}} = [b_x b_y b_z]^T$ between two vehicles is a vector in space expressed in a global coordinate frame (earth-centered, earth-fixed - ECEF). Each double difference measurement $\nabla\Delta\rho_{ij}^{kl}$ is a projection of the baseline vector $\tilde{\mathbf{b}}$ in the direction of the differenced satellite vector $\tilde{\mathbf{u}}^{\mathbf{kx}}$.

$$\tilde{\mathbf{u}}^{\mathbf{kx}} = \tilde{\mathbf{u}}^{\mathbf{k}} - \tilde{\mathbf{u}}^{\mathbf{x}} = \tag{7}$$

By taking three or more double difference measurements the baseline coordinates can be computed by resolving the following system of equations:

$$\begin{bmatrix} u_x^{kl} & u_y^{kl} & u_z^{kl} \\ u_x^{km} & u_y^{km} & u_z^{km} \\ u_x^{kn} & u_y^{kn} & u_z^{kn} \end{bmatrix} \begin{bmatrix} b_x \\ b_y \\ b_z \end{bmatrix} = \begin{bmatrix} \nabla\Delta\rho_{ij}^{kl} \\ \nabla\Delta\rho_{ij}^{km} \\ \nabla\Delta\rho_{ij}^{kn} \end{bmatrix} \tag{8}$$

A. Noise contribution in double difference measurements

Each double difference noise component in Eq. 6 $\nabla\Delta\tau_{\epsilon}$ includes the noise contributions from four pseudorange measurements, ρ_i^k, ρ_j^k, ρ_i^l and ρ_j^l. As subtraction cancels any common noise component out (e.g. noise at the antenna's LNA), we can work under the assumption that the noise of the different pseudoranges is statistically mutually independent of each other. The next equations present an example for two receivers i and j and three common satellites, k, l and m. The $\mathbf{L}$ matrix represents the linear relationship between the the pseudorange vector ρ and the double difference vector $\nabla\mathbf{\Delta}\rho$.

$$\nabla\mathbf{\Delta}\rho = \begin{bmatrix} \nabla\Delta\rho_{ij}^{km} \\ \nabla\Delta\rho_{ij}^{kl} \end{bmatrix} = \mathbf{L} \begin{bmatrix} \rho_i^k \\ \rho_i^l \\ \rho_i^m \\ \rho_j^k \\ \rho_j^l \\ \rho_j^m \end{bmatrix} = \begin{bmatrix} 1 & 1 \\ -1 & 0 \\ 0 & -1 \\ -1 & -1 \\ 1 & 0 \\ 0 & 1 \end{bmatrix}^T \begin{bmatrix} \rho_i^k \\ \rho_i^l \\ \rho_i^m \\ \rho_j^k \\ \rho_j^l \\ \rho_j^m \end{bmatrix} \tag{9}$$

$$\mathbf{R}_{\nabla\mathbf{\Delta}\rho} = \mathbf{L} \begin{bmatrix} R_{\rho_i} & 0_{(n+1)\times(n+1)} \\ 0_{(n+1)\times(n+1)} & R_{\rho_j} \end{bmatrix} \mathbf{L}^T \tag{10}$$

$$\mathbf{R}_{\rho_\mathbf{i}} = \sigma_\rho^2 \mathbf{I} \tag{11}$$

$$\mathbf{R}_{\nabla\mathbf{\Delta}\rho} = 2\sigma_\rho^2 \begin{bmatrix} 2 & 1 \\ 1 & 2 \end{bmatrix} \tag{12}$$

From Eq. 12 we learn that the the noise variance for a double difference measurement is four times the noise variance of each pseudorange measurement (assuming equal variance on all pseudorange measurements). Further on, it should be noticed that the resulting double differenced observations involving a common satellite are statistically dependent. Therefore, the calculated remaining noise covariance matrix $\mathbf{R}_{\nabla\mathbf{\Delta}\rho}$ is not diagonal, but has off-diagonal components of twice the noise variance of the pseudorange measurement.

B. Receiver Synchronization

When computing double differences, the pseudorange measurements have to be taken at the same time instant. Usually the GNSS receivers make the measurement at every whole second according to GPS time or a given fraction of a second according to its measurement rate. However, the receiver clock has a certain bias with respect to GPS time and this offset changes according to the clock drift of the internal oscillator. This means that measurements taken at two different receivers will usually have an offset of a few milliseconds, thus causing a partial uncorrelation of common errors. Eq. 13 explicitly shows this offset in measurement time from Eq. 5.

$$\begin{aligned} \nabla\Delta\rho_{ij}^{kl}(t) = \nabla\rho_i^{kl}(t) - \nabla\rho_j^{kl}(t+\Delta t) = \\ \rho_i^k(t) - \rho_j^k(t+\Delta t) - \rho_i^l(t) + \rho_j^l(t+\Delta t) = \\ R_i^k(t) - R_j^k(t+\Delta t) - R_i^l(t) + R_j^l(t+\Delta t) + \\ \tau_i^k(t) - \tau_j^k(t+\Delta t) - \tau_i^l(t) + \tau_j^l(t+\Delta t) \end{aligned} \tag{13}$$

The term $\tau_i^k(t) - \tau_j^k(t+\Delta t)$ will effectively cancel out the contributions towards satellite k coming from the atmosphere and the satellite given both, the proximity assumption and the assumption that these errors change slowly with respect to Δt. The same holds for satellite l. The term $\tau_i^k(t) - \tau_i^l(t)$

will completely cancel out the receiver i clock bias. Multipath errors, on the other hand, in general remain unsubtracted due to their low spatial and temporal correlation. Satellite, receiver, reflector or scatter movement cause the multipath characteristics to be time variant [19]. The initial assumption that $\nabla\Delta\tau_{error} \approx \nabla\Delta\tau_{mp} + \nabla\Delta\tau_{\epsilon}$ holds in the case of unsynchronized receivers.

Now, the third line in Eq. 13 contains the geometric ranges to the satellites k and l from receivers i and j. These could be rewritten as

$$\begin{aligned}\Delta R_{ij}^{k}(t) - \delta\Delta R_{ij}^{k}(\Delta t) - \Delta R_{ij}^{l}(t) + \delta\Delta R_{ij}^{l}(t+\Delta t) = \\ \nabla\Delta R_{ij}^{kl} - \delta\Delta R_{ij}^{k}(\Delta t) + \delta\Delta R_{ij}^{l}(t+\Delta t)\end{aligned} \quad (14)$$

The first term in the second line is the term we are interested in, representing the projection of the baseline at time t towards satellites k and l. The second and the third term represent the change in geometric range in Δt. The movement of the satellites during the offset time (and to a smaller extend the receiver's movements and the Earth's rotation) create a systematic error that has to be accounted for. The maximum relative movement between receiver and satellite is about 1000 m/s, leading to a double difference error of about one meter per every millisecond offset.

To correct these errors the receivers need to compute their clock offset and share the precise moment when the pseudorange, phase and Doppler measurements were taken. The clock offset is typically computed when estimating the receivers position by taken into account four or more pseudoranges.

We propose a technique to synchronize the measurements taken by different receivers at different time instants by performing a linear extrapolation of the pseudoranges using the pseudorange rate or Doppler measurement at the receiver. Eq. 15 shows the followed approach.

$$\rho(t_0 + \Delta t) = \rho(t_0) + \Delta t \cdot \lambda \cdot \dot{\phi}(t_0) \quad (15)$$

In Eq. 15 λ is the L_1 wavelength. The Doppler measurement at t_0 $\dot{\phi}(t_0)$ gives an estimate of the pseudorange change rate and can therefore be used to predict the pseudorange in $t_0 + \Delta t$. The extrapolation assumption holds as long as the relative movement between receiver and satellite is constant for this short period of time. The apparent Doppler shift caused by the receiver's clock drift is common to all satellites and will cancel out when double differencing.

In order to be able to perform this adjustment, the exact time t_0 when the measurement has been performed has to be known. The receiver will output the GPS timestamp at which the measurement is taken. This has to be corrected by the receiver clock offset, which the receiver is able to estimate by solving the navigation equations. The extrapolation time Δt is the difference to the next measurement epoch agreed by all participants. All measurements in the next section have been synchronized using this method.

Any change in speed, i.e. acceleration in vehicle and/or satellite will cause an erroneous extrapolation. Taking into account maximum vehicle accelerations of around 8 m/s², the range error due to a change in the vehicle's speed during 10 ms is in the order of micrometers and can be neglected. The change of the satellite's speed is below 1 m/s² and thus also be neglected. Therefore extrapolating using the Doppler measurement seems to be reasonable.

C. Communication Load

A brief analysis on the requirements on the communication channel comparing both, the exchange of raw data and the exchange of absolute position information, will follow next.

Based on the previous theoretical baseline computation the vehicles have to exchange the pseudoranges measured towards the satellites along with the corresponding Space Vehicle ID. Using 4 Bytes for each pseudorange measure, millimeter precision can easily be achieved. With the current GPS constellation consisting of 32 satellites, a receiver on the ground at medium latitudes is able to track a maximum of 13 GPS satellites. The usage of low elevation satellites is not recommended due to their greater atmospheric delay and their susceptibility to suffer stronger multipath [13]. The pseudoranges are assumed to have been extrapolated by the clock offset to the nearest point in the common time grid. This timestamp has to be exchanged in order to precisely align the pseudoranges in different cars. The time of week consists of the seconds passed since midnight Saturday/Sunday GPS time. Taking into account that the proposed relative positioning system will work in real time, it is not necessary to transmit the whole integer of seconds of week, a number that can grow up to 604800 and would require 20 bits for transmission. Assuming a minimum CAM transmission rate of 1Hz [2], it is sufficient to transmit the last bit of the second of week to unambiguously relate the measurements at the transmitter. Another 10 bit can be used for the fractional part in ms for measurements performed at higher rates than 1 Hz. Thus, for instance, a device producing raw data at 4Hz could timestamp the data in the following way: 0.250, 0.500, 0.750, 1.000, 1.250, 1.500, 1.750, 0.000, 0.250, etc.

This way, the maximum amount of data needed to be exchanged in every CAM message for pseudorange differentiation would yield 427 bit or 54 Bytes. Compared to the 14 Bytes needed to transmit latitude, longitude, altitude and timestamp values in the current CAM standard, the proposed approach needs four times more Data.

IV. Zero-Baseline Experiment

A zero-baseline experiment consists of two receivers which are fed with exactly the same GNSS signal received at one common antenna. By using an RF splitter the output of the antenna is guided to two receivers. This setup forces a zero-baseline between the receivers, making it an ideal experiment to validate the presented differencing and synchronization algorithms. At the same time it represents the best possible solution that can be achieved with two receivers, as the configuration forces all allegedly common errors to be equal (i.e. satellite and atmospheric errors) and therefore canceling out completely. In an ideal case one could assume that noise and

multipath could also cancel out completely, as the same signals are applied to both receivers. Nevertheless, the following deviations from the ideal zero-baseline experiment might have an impact on the resulting baseline not being zero.

- Receiver unsynchronization.
  As the receivers take pseudorange measurements at different points in time the white noise at the input of each receiver is not correlated and thus not canceling out. Possible multipath contributions are also less correlated the larger the time offset.
- Quantization Noise.
  After downconversion from RF to intermediate frequency an analogue to digital converter samples the incoming analogue signals and outputs digital samples. This process involves a quantization step that assigns to each output sample the nearest discrete value, thus producing quantization noise. As both receivers are not synchronized with each other, this noise signal is not correlated and will not cancel out.
- Receiver Response.
  The receiver automatically adapts the carrier and code loop filters to get the best trade-off between tracking accuracy and signal dynamics response. In some cases this response can be configured, but in general it is not visible to the user. Two independent receivers could respond differently to the same input.

Our intention is to analyze the response of our double difference approach to different error sources in a controlled environment. In our test setup two *ublox LEA 4T* receivers are connected through an RF-splitter to the output of a Spirent GSS7790 GNSS constellation simulator. Each antenna input is DC-blocked to prevent the antenna supply component damaging the Spirent simulator. The *ublox* receivers were configured with an automotive platform model and were set to output raw GPS measurements at 4 Hz. The Spirent simulator is able to simulate the GPS L_1 and L_2 signals arriving from a certain constallation of satellites to a virtual antenna located at a specific position at a specific point in time. The *ublox* receivers connected to the simulator will acquire and track the different signals, decode the navigation message and estimate its position, time and velocity. The SimGen software has been used to setup different test scenarios. SimGen enables to vary the power level of the signals of single satellites. Different errors, including atmospheric, satellite ephemeris and satellite clock errors and multipath, can be activated. Also the movement of the receiver antenna can be simulated by using a predefined ground vehicle motion model. In the following we show the results from a series of measurements with this zero-baseline configuration.

A. Static Scenario - No errors

In this scenario a static position of the receivers is simulated. First with a set of geostationary satellites and second with a regular constellation of GPS satellites. All satellite and atmospheric errors are deactivated. With this setup we aim at validating the double differencing technique with Doppler extrapolation proposed in section III-B. Fig. 3 and Fig. 4 show the pseudorange double differences and their mean and standard deviation over a period of 40 minutes.

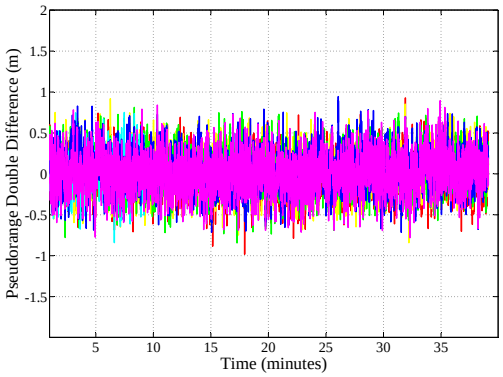

Fig. 3. Pseudorange double differences in a zero-baseline test setup. Each of the five colors represents one double difference to a different satellite and the common satellite.

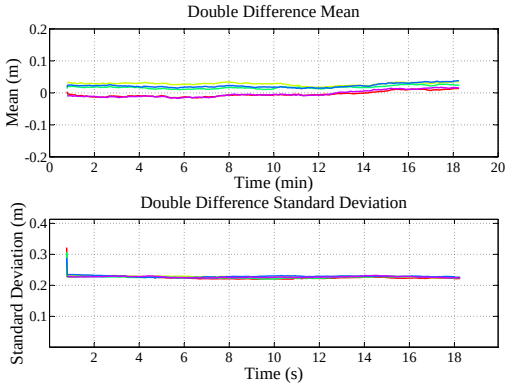

Fig. 4. Mean and standard deviation for code double differences. The mean for all five satellites is below 3 cm while the standard deviation is below 30 cm. The window length is 1250 s.

The figure shows that the mean values of the signals are zero for all double differences, as expected in a zero-baseline experiment. A random error corresponding to the noise on all four double differences still remains in the signal. The standard deviation for this error is below 30 cm. To further assess this random error in the code double differences, during the test the signal power of the satellites was decreased stepwise from +20 dB to -5 dB with respect to -130 dB nominal power. A low carrier-to-noise density leads to a higher variance in the pseudorange measurement. This dependence is receiver dependent and is a function of the bandwidth of code tracking loop, the integration time and the early-late correlator spacing among other parameters and can be expressed in general by the following equation [13], [20]:

$$\sigma_{\rho_i} = 4 \cdot c \cdot T_c \sqrt{\frac{C}{\frac{C}{N_0}}} \tag{16}$$

Fig. 5 shows this relationship. A curve fitting of the sample points to the general form yields the parameter C = 7.5e-4. This relationship is valid for these receivers and under the

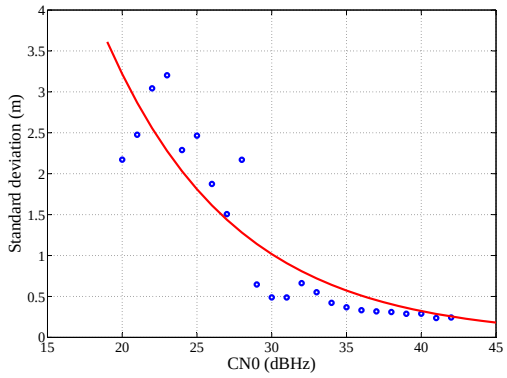

Fig. 5. Pseudorange double difference standard deviation vs. $\frac{C}{N_0}$ in a zero-baseline experiment. The error in the double differences grows with decreasing carrier-to-noise ratio in both satellites.

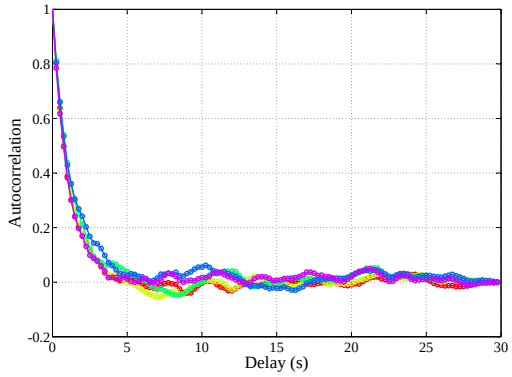

Fig. 6. Autocorrelation function of five different pseudorange double differences. A time correlation of about 4 s can be observed.

assumption that the parameters of the tracking loops do not change over time.

Further on, the time correlation of the double differences is analyzed. Fig. 6 shows the autocorrelation for the code double differences in time. The double differences have a time correlation of approximately 4 seconds, yielding a delay-locked-loop (DLL) bandwidth of 0.25 Hz.

For future analysis it is as well important to analyze the statistical distribution of the error and to know if the assumption of a Gaussian distribution for the noise in the code double differences holds. Fig. 7 shows a histogram of the amplitude of the double difference signals. Although the shape of the histogram could suggest the remaining noise to be modeled according to a normal distribution, a Kolmogorow-Smirnow normality test rejects the hypothesis of Gaussian noise.

B. Static Scenario - Common errors

To demonstrate the correct cancellation of common errors in the code double differences an atmospheric delay has been modeled using the Spirent simulator. An ionospheric delay τ_{ion} is modeled choosing a set of parameters for the Klobuchar

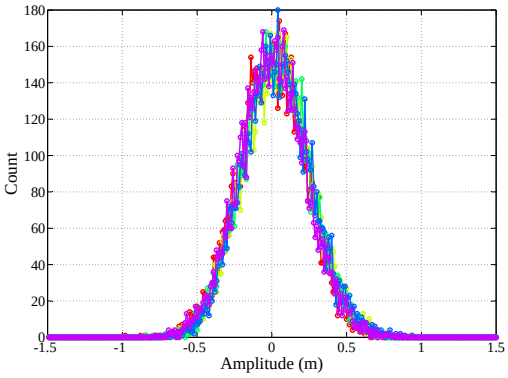

Fig. 7. Histogram of the amplitude of the pseudorange double differences.

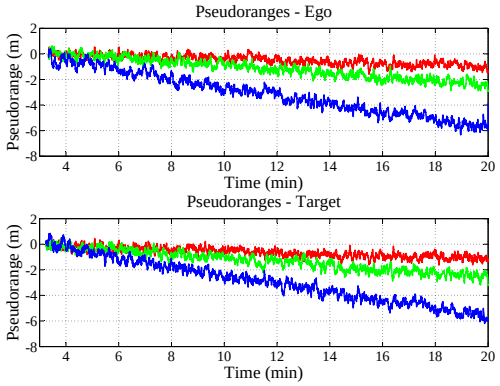

Fig. 8. Pseudorange to satellites 8, 9 and 24 at both receivers. The changing delay is caused by the modeled ionospheric and tropospheric delays.

model [21] that are applied on the RF signals. The error is different on each satellite and varies over time. The delay caused by the simulated ionosphere ranges from 2.14 m to 11.25 m. Additionally, a tropospheric delay τ_{trop} is simulated using a tropospheric model specified in STANAG 4294 [22]. This causes a delay ranging from 2.7 m to 27.5 m. Fig. 8 shows the pseudorange signal to three satellites. In order to be able to visualize the pseudoranges correctly, the initial offset is subtracted and the temporal variation due to satellite movement and user and satellite clock is corrected integrating the carrier phase of the signal. It can be clearly seen how the pseudoranges show a varying delay that can only be caused by the atmospheric delay. While the satellite moves, the delay changes due to the different propagation of the signal through the atmosphere. The double differences $\nabla\Delta\rho_{ij}^{kl}$ in Fig. 9, however, do not show any increased error or offset. The variance of the signal and its mean show similar values as in the previous error-free scenario.

C. Static Scenario - Multipath errors

In order to assess the impact of multipath, three different multipath models haven been simulated, namely a *fixed offset multipath model*, a *Doppler offset multipath model* and a *ground reflection multipath model*.

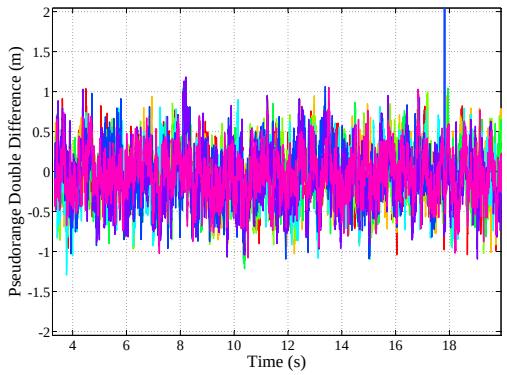

Fig. 9. Pseudorange double differences in zero-baseline setup in the presence of ionospheric delay. The ionospheric delay modeled on the SV's signals varies from 2 m to 12 m.

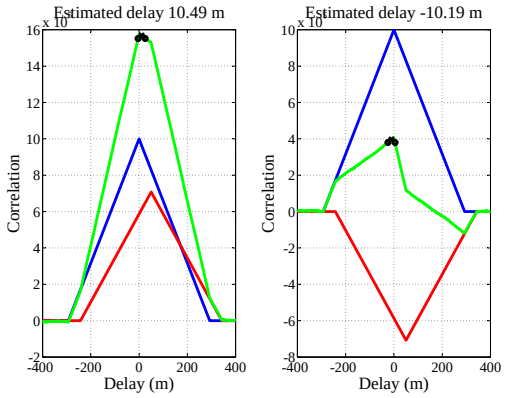

Fig. 10. Pseudorange error in the code correlator produced by a second 3 dB attenuated and 50 m delayed path with phase delay zero (left) and π (right). The direct path is represented in blue and the delayed path is represented in red. The green curve represents the code correlator output (early-late spacing is 0.1 chip and integration time is 1 ms.)

The *fixed multipath model* simulates a second delayed replica of the PRN code on a separate channel. The delay of the second signal affects both the code and the phase of the carrier, however, in this model this initial offset stays constant over time. A different phase offset causes a different interference between both paths. Fig. 10 shows the interference for a phase offset of zero and π between the direct path (blue) and the a second path (red) with 50 m delay and 3 dB attenuation. The resulting error varies from about 10 m to -10 m. Different time delays for the second path, with different relative phase and different loss has been simulated using the Spirent simulator in order to analyze its impact on the double differences. The assumption is that the fixed and time invariant offset will bias in the same way both receivers and will cancel out when performing double differences. Fig. 11 shows the measured pseudoranges for three satellites at both receivers. Different steps every three minutes correspond to a change in the delay of the second path. From minute 10 to minute minute 37 an offset of around 10 m and phase delays from 0 to 2 π have been simulated. Then the delay increases stepwise to approximately 50 m until minute 55. From minute 55 on a delay of approximately 10 m and decreasing loss of the second path is simulated. At first glance both receivers act in the same way. Fig. 12 show the code double differences for the same set of satellites.

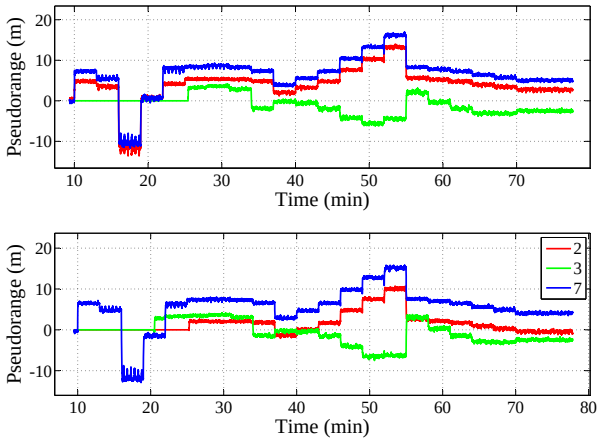

Fig. 11. Pseudoranges for SV 2,3 and 7 at ego and target receiver with a fixed offset model. The curves at zero at the beginning of the simulation are satellites that are still not acquired. From minute 10 to 37 a delay of around 10 m and varying phase offset is simulated. From minute 37 to minute 55 the offset is increased stepwise from 1 m to 50 m. From minute 55 an offset around 10 m is decreased in loss from 1 dB to 12 dB.

Surprisingly, the double differences are biased by a certain amount indicating that the fixed offset is not completely canceled out after differentiation. Nevertheless, the figure shows that this bias is small in relation to the offset of the second path. This indicates that although the receivers are of the same model each of them gives a slightly different estimate in the presence of a reflection.

The *Doppler multipath model* is an extension of the fixed multipath model, where the delayed and attenuated second path has a Doppler offset with respect to the direct path. The Doppler offset produces a change in the phase of the second path, and this way changes the sign of the interference periodically. Depending on the Doppler offset the tracking loops are able to track this periodic change or might only show an offset in the pseudoranges. Doppler offsets ranging form 0.1 Hz to 200 Hz have been simulated every three minutes starting at

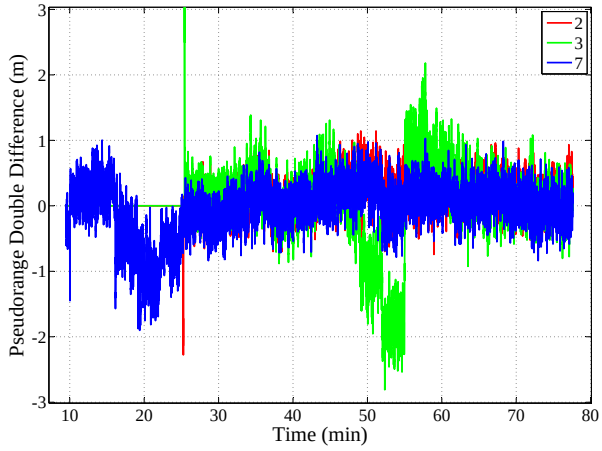

Fig. 12. Pseudoranges double differences for satellites 2,3 and 7 with a fixed offset multipath model.

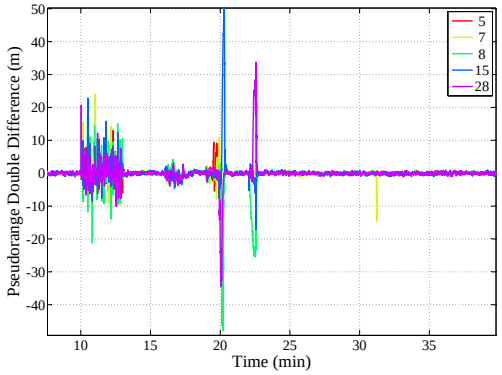

Fig. 13. Pseudorange double differences for several satellites with a Doppler multipath model. Different Doppler offsets ranging from 0.1 Hz to 200 Hz are simulated every three minutes starting from minute 10 on. The delay of the second path is 15 m and the attenuation 3 dB.

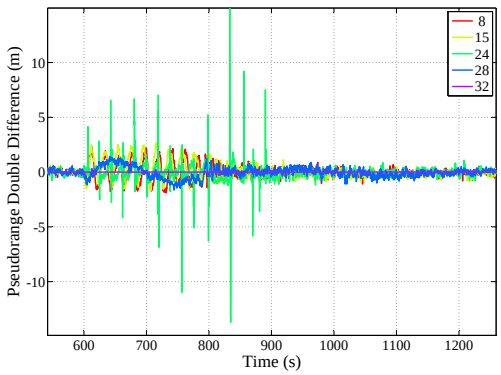

Fig. 14. Pseudoranges double differences for a descendent from 50 m to 0 m with ground reflection model activated. At 600 s the ground reflection multipath model is activated. At 780 s the descent starts. The variations in speed occur smoothly.

minute 10. These values would correspond to the Doppler shift experienced by a receiver moving directly towards a reflector at a speed of 0.07 km/h and 137 km/h respectively. The second path has a delay of 15 m and an attenuation of 3 dB. Fig. 13 shows the resulting double differences.

The Doppler offset of 0.1 Hz creates periodic disturbances to the double differences every 10 s. This disturbance is created when both paths interfere negatively and the signal vanishes. This could be verified by looking at the $\frac{C}{N_0}$ over time graph for both receivers, where a periodic interference pattern could be recognized. A Doppler offset of 1 Hz does not seem to be harmful. At 16 minutes the 5 Hz Doppler is activated and meter disturbances occur to all double differences that get smaller after two minutes. The 10 Hz and 30 Hz Doppler shifts generate errors in Double Differences of up to several tenths of meters. But after a one two and one minute respectively they converge again to the true baseline. High Doppler shifts (80, 120, 160 and 200 Hz) do not seem to impact the double differences as they are averaged by the tracking loops.

The *ground reflection model* simulates a second path arriving at the antenna after reflecting on the ellipsoid. This test is somehow a combination of the previous two tests. In contrast to the fixed offset model, here the delay between the direct and the reflected path may change with the movement of the surrounding. This change in delay will create a Doppler offset between both paths. A static receiver at a certain height will experience a relatively slow interference due to the changing elevation of the satellite, which will create a changing interference pattern due to the changing phase offset. In this test we have changed the height of the antenna from 50 m to 0 m at 0.1 m/s, which correspond to Doppler offsets between the paths around 0.5 Hz. Fig. 14 shows the resulting code double differences for the descent. At 600 s the ground reflection model is activated, while at 780 s the descent starts.

From 600 s to 780 s a periodic interference can be observed, corresponding to the angular movement of the satellite. Here the Doppler offset is about 0.1Hz. We can see that errors up to 10 m are possible. The amplitude and the frequency of the error due to the interference is different for each satellite, depending on its elevation. From 780 s to 1250 s, the receivers

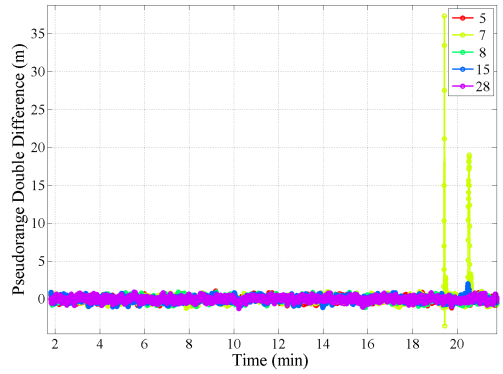

Fig. 15. Pseudorange double differences for several satellites in a dynamic test. The receivers experience high speeds up to 80 m/s and high accelerations up to 15 m/s². The signal towards a located satellite (SV 7) experiences a major error when performing the 15 m/s² acceleration.

descend from 50 m to 0 m. The descending speed is changed gradually from 0 m/s to 0.1 m/s and back to 0 m/s. This increasing speed creates a increasing Doppler offset between both paths, that produces a faster variation in the pseudorange errors. Eventually this interference is too fast to be tracked by the code tracking loop and the error is below the noise level.

D. Dynamic scenario

A dynamic scenario has been simulated, where the antenna recursively accelerates from standstill to a certain speed, moves at constant speed, decelerates back to zero and holds still for one minute. The accelerations simulated are 3, 5, 7 10 and 15 m/s² while the speed varies from 14 m/s to 80 m/s. The purpose of the test is to see if high vehicle dynamics can have an impact on the pseudorange double differences. Fig. 15 shows the pseudorange double differences for the dynamic scenario. It can be observed that the errors until minute 19 no errors occur on the double differences. The last acceleration of 15 m/s², however, has a major impact on the double difference towards satellite 7.

V. Conclusion

A method to compute pseudorange double differences using unsynchronized measurements at two receivers and performing a Doppler extrapolation has been presented. Its applicability to the vehicular environment has been discussed. A series of zero-baseline experiments with two *ublox LEA 4T* receivers have been performed in order to assess the performance of pseudorange double differencing in vehicular environments. The experiments have been performed in a controlled environment using a Spirent GSS7790 GNSS constellation simulator. The method to compute code double differences has been validated in a error-free environment. The remaining noise error from the receivers has been analyzed in terms of mean, variance, time correlation and amplitude distribution. The correct cancellation of common errors in both receivers has been successfully shown by simulating an atmospheric delay on different satellites. The code double differences resulting from this experiment are free of any possible bias. In a second set of experiments the double difference signals are evaluated under the effect of multipath propagation. Different multipath models show that multipath is not canceled by double differencing. Static multipath components at both receivers show small errors of below two meters. Time varying multipath, however, is capable of creating large errors in double differences. High dynamics in speed and acceleration, on the other hand, behave as expected when differencing and yield a baseline of zero length. The practical application of double differencing for baseline estimation for vehicle relative positioning, requires to place one antenna on each vehicle. Future studies will examine the potential of double differencing for relative position estimation in real world.

References

[1] F. de Ponte Müller, L. M. Navajas, and T. Strang, "Characterization of a laser scanner sensor for the use as a reference system in vehicular relative positioning," in *Communication Technologies for Vehicles*, pp. 146–158, Springer Berlin Heidelberg, 2013.

[2] ETSI TS 102 637-2, "Intelligent Transport Systems (ITS) - Vehicular Communications - Basic Set of Applications - Part 2 : Specification of Cooperative Awareness Basic Service," tech. rep., ETSI, 2010.

[3] E. Richter, M. Obst, R. Schubert, and G. Wanielik, "Cooperative relative localization using vehicle-to-vehicle communications," in *Information Fusion, 2009. FUSION '09. 12th International Conference on*, pp. 126 –131, july 2009.

[4] N. Alam, A. Tabatabaei Balaei, and A. G. Dempster, "Relative positioning enhancement in vanets: A tight integration approach," *Intelligent Transportation Systems, IEEE Transactions on*, vol. PP, no. 99, pp. 1 –9, 2012.

[5] D. Yang, F. Zhao, K. Liu, H. B. Lim, E. Frazzoli, and D. Rus, "A GPS Pseudorange Based Cooperative Vehicular Distance Measurement Technique," in *VTC Spring*, pp. 1–5, IEEE, 2012.

[6] C. Han, S. Lee, Y. Kim, J. Song, H. No, and C. Kee, "GPS/IMU Integrated Relative Positioning for Moving Land Vehicles with V2V (Vehicle-to-Vehicle) Communication Module," in *Proceedings of the 25th International Technical Meeting of The Satellite Division of the Institute of Navigation (ION GNSS 2012)*, pp. 636 – 641, 2012.

[7] M. Yang, "Noniterative method of solving the GPS double-differenced pseudorange equations," *Journal of Surveying Engineering*, vol. 131, no. 4, pp. 130–134, 2005.

[8] J. G. García, P. I. Mercader, and C. H. Muravchik, "Use of GPS carrier phase double differences," *Latin American applied research*, 2005.

[9] N. Alam, A. Balaei, and A. Dempster, "Positioning enhancement with double differencing and dsrc," in *Proceedings of the 23rd International Technical Meeting of The Satellite Division of the Institute of Navigation (ION GNSS 2010)*, (Portland, OR), pp. 1210–1218, September 2010.

[10] Z. Li and H. Leung, "Gps/ins integration based navigation with multipath mitigation for intelligent vehicles," in *Mechatronics, ICM2007 4th IEEE International Conference on*, pp. 1–5, 2007.

[11] J. Farrell and M. Barth, *The Global positioning system and inertial navigation*. McGraw–Hill, 1999.

[12] J. Farrell and T. Givargis, "Differential gps reference station algorithm - design and analysis," 2000.

[13] E. Kaplan, *Understanding GPS - Principles and applications*. Artech House, 2nd edition ed., December 2005.

[14] O. Le Marchand, P. Bonnifait, J. Ibanez-Guzman, D. Betaille, and F. Peyret, "Characterization of GPS multipath for passenger vehicles across urban environments," *ATTI dell'Istituto Italiano di Navigazione*, pp. 77–88, 07 2009.

[15] S. Zeng, "Performance Evaluation of Automotive Radars Using Carrier-Phase Differential GPS," *IEEE Transactions on Instrumentation and Measurement*, vol. 59, pp. 2732–2741, Oct. 2010.

[16] N. Luo, "Precise relative positioning of multiple moving platforms using GPS carrier phase observables," 2001.

[17] N. Luo and G. Lachapelle, "Relative positioning of multiple moving platforms using GPS," *Aerospace and Electronic Systems, IEEE Transactions on*, vol. 39, no. 3, pp. 936–948, 2003.

[18] C. C. Kellum, "Basic Feasibility of GPS Positioning without Carrier-Phase Measurements as a Relative Position Sensor between Two Vehicles," in *Proceedings of the 2005 National Technical Meeting of The Institute of Navigation*, pp. 903 – 910, 2005.

[19] A. Lehner, A. Steingaß, and F. Schubert, "A novel channel model for land mobile satellite navigation," *ATTI Journal dell'Istituto Italiano di Navigazione* , pp. 108 – 119, 2009.

[20] P. Misra and P. Enge, *Global Positioning System: Signals, Measurements, and Performance*. Ganga-Jamuna Press, Lincoln MA, 2nd edition ed., 2006.

[21] J. Klobuchar, "Ionospheric time-delay algorithm for single-frequency gps users," *Aerospace and Electronic Systems, IEEE Transactions on*, vol. AES-23, no. 3, pp. 325–331, 1987.

[22] North Atlantic Treaty Organization, *NATO Standard Agreement STANAG 4294 Issue 1*, 1993.